Clays and Clay Minerals, Vol. 43, No. 4, 446–454, 1995.

A (1:1) 7-Å Fe PHASE AND ITS TRANSFORMATION IN RECENT SEDIMENTS: AN HRTEM AND AEM STUDY

MARC AMOURIC,[1] CLAUDE PARRON,[2] LIONEL CASALINI,[2] AND PIERRE GIRESSE[3]

[1] Centre de Recherche sur les Mécanismes de la Croissance Cristalline
CRMC2-CNRS, Campus de Luminy, case 913
13288 Marseille Cedex 9, France

[2] Laboratoire de Géosciences de l'Environnement-URA CNRS 132
Université d'Aix-Marseille III, 13397 Marseille Cedex 20, France

[3] Laboratoire de Sédimentologie Marine, Université de Perpignan
Av. de Villeneuve 66025 Perpignan, France

Abstract—Young marine green grains, from Fe-rich sediments, were studied by using HRTEM systematically combined with punctual microchemical EDX analyses. Experimental results demonstrated these grains were made of a mixture of very small phases (mainly 1:1 and 2:1 silicates layer phases) with a dominant 7-Å Fe specie. All the main crystallochemically characterized phases appeared intimately related in the same evolutionary process. Each of them experienced different and well described conversion mechanisms. So first, a starting original Fe-rich kaolinite recrystallized via solution into another particular 7-Å Fe-rich phase, the composition of which varies from a di-tri to a pure trioctahedral (Mg + Fe) end member.

This Fe-rich 1 : 1 mineral is effectively not a classical one. Then crystallization of a 10Å, rather dioctahedral K-rich phase occurs at the expense of it, through 1:½:1 interstratified structures. Such an evolution takes place through a solid state mechanism in which one 10-Å layer replaces one 7-Å layer. Another part of mica-like structures may also directly develop after dissolution of original kaolinites. The development of 10-Å K-rich phases could be significative of the beginning of the glauconitization process in these grains.

Key Words—7-Å Fe phase, 10-Å phyllosilicates, AEM, HRTEM, Marine sediments, Phase transformation.

INTRODUCTION

In recent marine deposits, on many shallow marine shelfs, green peloïds containing Fe-silicates occur in tropical latitudes. Formation of these peloïds is related to the content and mobility of Fe in the sediments. Near the mouths of the rivers, in the zones of high sedimentation, they are essentially made of Fe-bearing 7-Å phyllosilicates. Such an occurrence has already been reported in numerous papers but related analytical results and mineralogical conclusions were quite different. Briefly, the main 7-Å Fe phase detected was successively identified first as "chamosite," then as "Berthierine" and lastly as "Odinite" (Phyllite V) (see, e.g., Von Gaertner and Schellman 1965, Porrenga 1967, Odin and Giresse 1972, Odin and Matter 1981, Giresse *et al* 1988, Odin *et al* 1988). According to these papers, it appears today that even if progress has been realized during the last years, fundamental data about the 7-Å Fe phase such as its nature, its origin and formation mechanisms and its meaning are still controversial. A great part of these problems probably are due to the fine mixture of phases often encountered coexisting with the 7-Å Fe one, even after careful and various purification treatments, to the very small size of all these phases present and to the global aspect of the analytical methods generally used in the previous studies (X-rays; microprobe analyses, . . .) to characterize such a material.

In this work, to obtain the most precise structural and chemical results as possible about the 7-Å Fe phase and accompanying other ones, and for a better understanding of the mineral processes which take place in corresponding green peloïds, we simultaneously used high resolution transmission electron microscopy (HRTEM) and energy dispersive X-ray spectrometry (EDXS) at a ten-nanometers-scale. We have focalized on one sample which was given us by Giresse. Collected 45 km NW of the Congo estuary, it was labelled "191-7G" and classified by Giresse *et al.*(1988) as the richest in the 7-Å Fe phase among the samples from recent deposits of this river. The massive formation of Fe-bearing 7-Å phases in the green peloïds was estimated to take 10^2 to 10^3 years (Giresse 1985).

EXPERIMENTAL PROCEDURES

Sample 191-7G was derived from an area of 7-Å minerals containing 20–30% Fe_2O_3 and 2–3% C_{org}. Previously, Giresse *et al* (1988) had selected it by densitometry, then studied it by X-ray diffraction method, microprobe and Mössbauer analyses. Briefly, their X-ray diffraction (XRD) data have shown this sample was the purest in the 7-Å Fe phase characterized by a

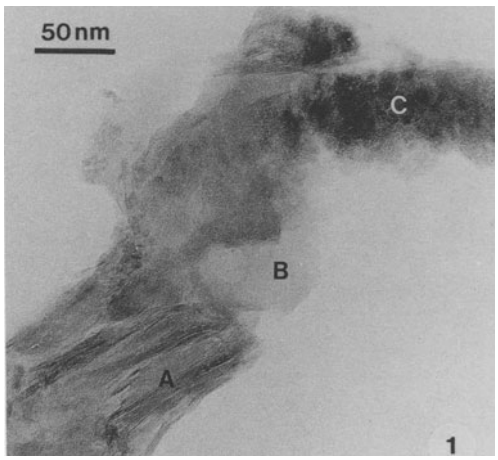

Figure 1. Wide field transmission electron micrograph showing intimate structure of green grains with Fe-phyllosilicates (a), a probable kaolinite (b) and a granular Fe-rich gel-like material (c).

particular (060) reflection at 1.52 Å and might contain some goethite and quartz. Chemically, as from XRD data, they concluded that the structural Fe-in the 7-Å Fe phase-was mostly divalent.

For HRTEM study, we have embedded the same sample in araldite resin before sectioning it on an ultramicrotome equipped with a diamond knife. A JEOL 2000 FX (200 KV) electron microscope, equipped with an objective lens pole piece with an aberration coefficient Cs ~2.3 mm, was used for observations. Reflections passing through a 50-μm objective aperture centered on the incident 000 beam contributed to the images which permitted a ~3 Å point to point resolution. Images were selected from experimental through-focus series recorded in the 800–1200 Å range of underfocusing. The optimal imaging conditions for phyllosilicates were defined referring to previous image simulations in micas (Amouric *et al* 1981). To avoid possible electron-beam damage to the specimen, tilting procedures were not used. As a result, quickly recorded one dimensional images were mainly analysed in this work. However most of these images showed characteristic 00l lattice fringes of the dominant mineral phases present in the sample. Simultaneously, we have done EDX analyses on the same sample. That means that, systematically, one or several "fine" (about 10 nanometers scale) microchemical analyses were recorded, directly coupled with each interesting and well identified structure image observed in HRTEM. A Tracor system (TN 5502) equipped with a Si(Li) detector was used. For a good correlation between structure images and local chemical analyses, beam probes 50 to 200 Å in diameter with constant beam current were chosen throughout the study. Collected data were processed by a program based on the Cliff and Lorimer method (1975) and using appropriate layer silicate standards.

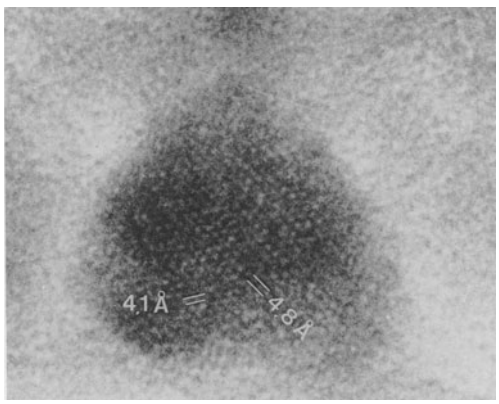

Figure 2. Structure image of one particule of the granular Fe-like gel (Fig. 1c). Note the 4.1 and 4.8 Å periodic spacings, characteristic of a goethite structure.

STRUCTURAL AND FINE-SCALE ANALYTICAL RESULTS

General texture

A wide field micrograph (Figure 1) taken at a mean direct magnification of 100.000, shows the intimate and characteristic organization of the main phases which occur in the sample (A, B, C zones). Several of them were previously unrevealed by XRD (Giresse *et al* 1988). So, zone A appears to consist of a spindle-shaped arrangement of layered crystallite packets. Such crystallites are generally thin, wavy and strongly diffracting as is, in details, the 7-Å Fe phase (see Figure 3). Zone B exhibits a large flake with a pseudo-hexagonal habit, similar to a phyllosilicate viewed along c*. Its corresponding chemical analysis and apparent very weak contrast suggest this phase strongly resembles a kaolinite. In zone C, an inhomogeneous, structurally non-organized, strongly diffracting and Fe-rich material is visible, similar to a gel.

The non-layered phases

At higher magnification, the gel-like material (zone C, Figure 1) consists of many finely divided particles more or less aggregated (Figure 2). Periodic spacings at 4.1Å and 4.8Å are visible on the structural image of such a (Fe)-particule. They are respectively interpreted as the (110) and the (020) planes of goethite. So, the gel-like material (Figure 1) is probably an organizing proto-goethite. Many small quartz grains, with a characteristic vitreous aspect and a weak contrast as also many rounded pseudo-quadratic anatase crystallites were observed. They were considered as inherited phases in this sample.

The layered phases

The 7-Å (1:1) phyllosilicates. Statistically, a pure 7-Å Fe phase with a spindle like arrangement was the more

https://doi.org/10.1346/CCMN.1995.0430408 Published online by Cambridge University Press

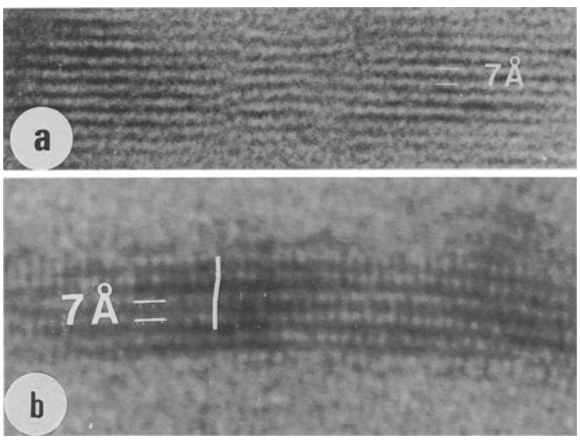

Figure 3. a) Lattice-fringe image of a thin lath of 7-Å Fe phase (Basal spacings d(001) ~ 7Å). b) Structure image of one crystallite of the 7-Å Fe phase showing its faulted 1M polytypic sequence viewed along [100] or [100].

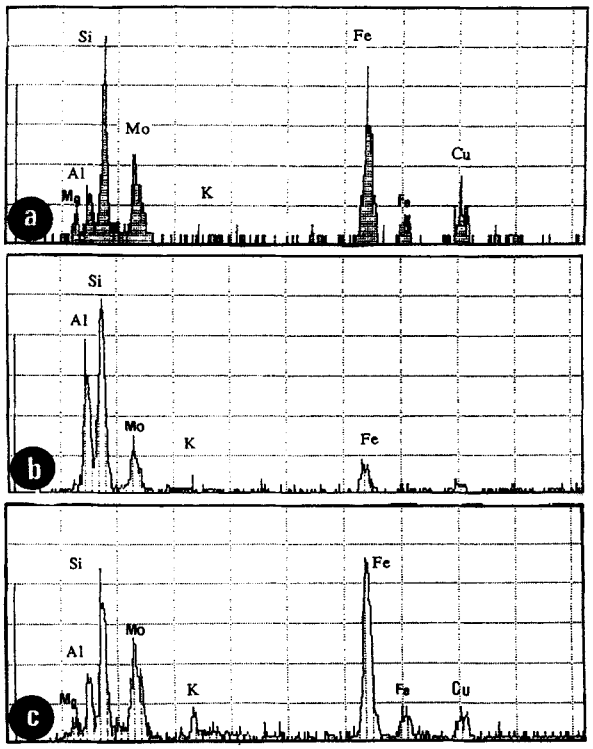

Figure 4. Microchemical analyses spectrum of a) the 7-Å Fe phase b) the 7-Å kaolinite like phase; c) the 10-Å mica like phase.

representative species (≥70%) detected in the studied peloïds (Figure 1). Each spindle is made of well-organized crystallites showing a 7-Å regular basal spacing (Figure 3a) and each crystallite consists of thin and flexible lath commonly 70–150 Å wide and about ten times longer. From a polytypic point of view, the 1M structure was as abundant as the 1Md (disordered) structure (Figure 3b). Corresponding qualitative and semiquantitative micro-chemical analyses always revealed a high and specific structural Fe-content (Table 1a and Figure 4a).

Another 7-Å 1:1 phase was observed. It was poorly represented (<5%) in this sample—probably as a relic—but always intimately mixed with the Fe-phase before. However its typical morphology, its chemistry and strongly damaged structure under the beam permitted it to be easily distinguished. Indeed, such a phase always occurred as very thick, short and regular laths (Figure 5) or as large flakes with a very weak contrast when viewed along c* (Figure 1, B zone). Polytypic sequences observed were generally of 1Md type or exhibited a repeated 21-Å periodicity (Figure 5) giving a probable 3Tc polytype. Coupled micro-analyses were also different. Results (Table 1b and Figure 4b) indicated a chemical composition close to kaolinite (high Al and poor Fe content). This was not surprising. Giresse *et al* (1988) have reported pure kaolinite as the main original specie present in the recent sediments studied before it evolved in a 7-Å Fe phase. However, they had not particularly detected kaolinite in this sample (191-7G) and, in fact, our HRTEM and EDX data could suggest the relic 7-Å Al phase we observed rather was a "Fe-Kaolinite" obtained after some Fe introduction in a kaolinite structure.

Table 1. Examples of EDX microchemical analyses normalized to 100 wt% of: a) the 7-Å Fe phase; b) the 7-Å kaolinite like phase; c) the 10-Å mica like phase; d) a 7/10 Å interstratfied sequence.

	a		b		c		d	
EL-LINE	ATOM%	EL WT%	ATOM%	EL WT%	ATOM%	EL WT%	ATOM%	EL WT%
SI–K	41.36	33.11	50.11	48.00	46.27	40.37	49.79	40.79
MG–K	13.77	9.45	3.73	3.06	7.22	5.40	6.81	4.78
AL–K	16.09	12.42	39.04	36.06	25.42	21.39	16.23	12.82
K–K	0.38	0.42	0.79	1.06	6.13	7.45	3.40	3.88
FE–K	26.65	42.67	5.67	10.85	13.61	23.75	21.23	34.79
CA–K	0.89	1.02	0.34	0.47	1.08	1.35	2.06	2.41
TI–K	0.13	0.17	0.25	0.42	0.00	0.00	0.10	0.15
CL–K	0.73	0.73	0.06	0.08	0.26	0.29	0.37	0.38

https://doi.org/10.1346/CCMN.1995.0430408 Published online by Cambridge University Press

Figure 5. Lattice-fringe image of a thick lath of a 7-Å phase (of kaolinite type). Note the regular 21Å basal spacing along c* of this particular polytypic sequence.

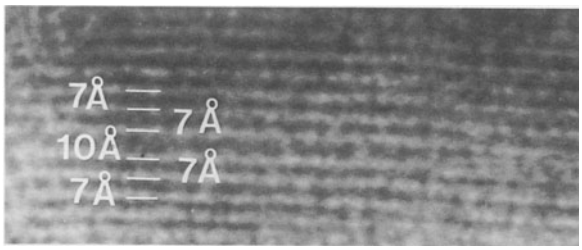

Figure 7. Lattice-fringe image of an irregular 7/10Å interstratified sequence along c*.

A pure 10-Å (TOT) phase. HRTEM observations revealed also several crystallites of another layered phase having 4–5 to 10–30 layers stacking along c*. They were structurally characterized by their 10-Å like mica basal spacings (Figure 6) and, chemically, chiefly by a specific higher K content (Table 1c, Figure 4c) compared to the other phases. Such a 10-Å phyllosilicate was unsuspected in this sample by Giresse *et al* (1988) and detected with HRTEM by Odin *et al* (1988) in a similar material but not precisely studied. However all these authors believed this 10-Å phase certainly occurred, but in more mature or ancient green peloïds.

7/10Å phases interstratification and lateral transition. In addition, details of HRTEM images have demonstrated that 7-Å and 10-Å layers could be mixed in a same crystallite of this sample, giving rise to various interlayered configurations. So a disordered interstratification was generally observed in this study, as illustrated in Figure 7, but different intermediate states between a pure 7-Å phase and an ordered sequence of 1/1 7–10 Å type (see Figure 8b, left part) existed also (Casalini *et al* 1993).

Such observed mixed structures were suggestive of a transformation process in progress. Furthermore, continuous lateral transitions of one unit 7-Å layer into one unit 10-Å layer (a 1:1 reaction) were frequently evidenced in the same specimen (Figure 8), with an obvious increasing volume. Such observations are consistent with a solid-state transformation mechanism and may concern large crystallites as micro-crystalline particles, as previously deduced from similar HRTEM images of mica chloritization for example (Olives and Amouric 1984) or for smectite to illite transformation in some cases (Amouric and Olives 1991). Note also that such 7–10 Å lateral transitions are very often observed developing in opposite directions, on several successive layers as shown in Figure 8a. Such an original situation probably lead to minimize and to homogenize in the mother 7-Å structure the global deformation energy due to this solid-state transformation. A detailed explanation of this configuration drawn in Figure 8 is that, due to an increase in volume, a local strain set up at the front of one developing mica-layer in the original 7-Å phase. This inhibited growth of an immediately adjacent mica layer in the same direction but growth of it in the opposite direction is possible. However two immediately adjacent and opposite growth fronts must block each other and in this

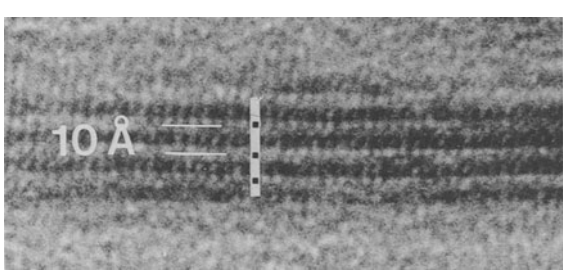

Figure 6. Structure image of 1M mica-like polytypic sequence viewed along [100] or [$\bar{1}$00]. (Basal spacing d(001 ~ 10Å.)

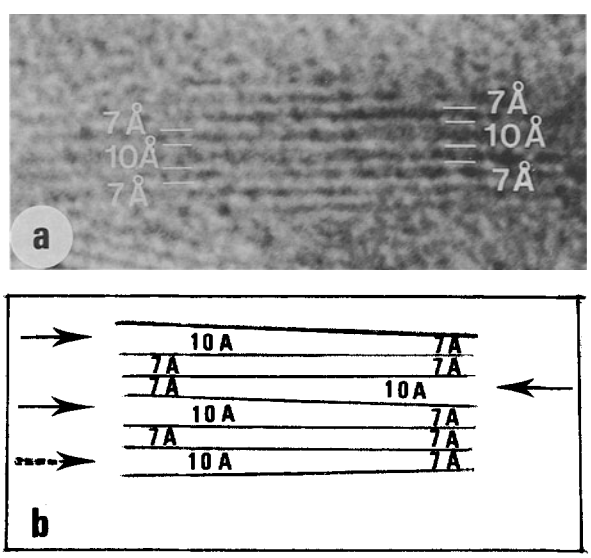

Figure 8. a) Lattice-fringe image of a rather regular 7/10Å interstratified structure along c*. Note the lateral transformation of one layer of the 7-Å Fe phase to one layer of 10Å-like mica phase within the (OO1) plane. b) Schematic representation of a).

https://doi.org/10.1346/CCMN.1995.0430408 Published online by Cambridge University Press

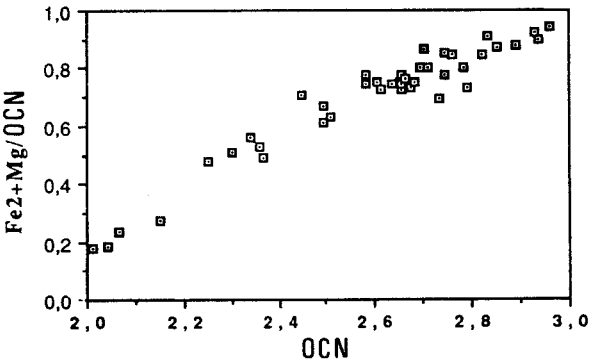

Figure 9. Variations of the (Fe^{2+} + Mg) cations ratio in octahedra as a function of the octahedral cations number (OCN) in the 1:1 phases group observed.

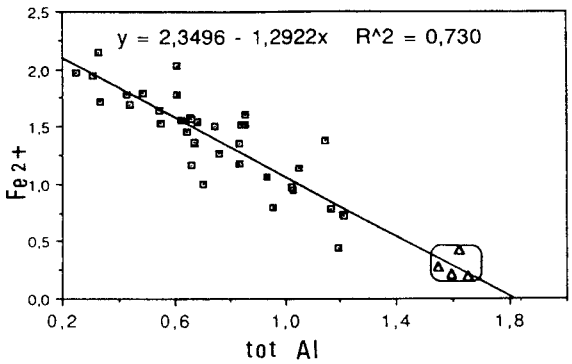

Figure 10. Variations of the Fe^{2+} content as a function of total Al in the 7-Å Fe phases. The field of the primary (Fe) kaolinite is shown on the lower right of the diagram.

case the lateral transformation remains uncomplete as illustrated in Figure 8a. So during the evident 7-Å phase–10Å phase lateral transition, the process may start at one end or simultaneously at both ends of 7Å crystallites, from the edges to the core of the crystallites with sometimes opposite transformation fronts slightly shifted which locally block the process. A relatively similar situation was described by Banfield and Eggleton (1988) for mica to vermiculite transition. However these authors did not observe just adjacent fresh vermiculite layers growing in opposite directions (but only vermiculite separated by about four or five biotite layers). They estimated such a separation was necessary before the supposed stress field around a first developing vermiculite layer had dissipated sufficiently. Certainly fields stress implied in our case were weaker and the TO structures as the soft sediments studied here globally were more easy to deform. Micro-chemical analyses of such interstratified structures gave varied and intermediate composition (Table 1d) between that of the 7-Å Fe phase (Table 1a) and the 10-Å phase (Table 1c). Such chemical data determined which 7-Å phase was interstratified and laterally transformed.

CRYSTALLOCHEMICAL RESULTS

EDX analyses can not distinguish between Fe^{2+} and Fe^{3+}. With limited sample material, we referred to the Mössbauer data of Giresse *et al* (1988) for this sample studied. So in the following we have considered that the total iron was mainly Fe^{2+} but we have also imposed total iron as Fe^{3+}, sometimes, for certain calculations. The structural formulae were established both on a 1:1 silicate layer (TO structure, with 7 oxygens) and on a basis of a 2:1 silicate layer (TOT structure, 11 oxygens). When all the microchemical analyses were taken into account, the Si content in the related structural formulae discriminated 3 phase-groups: 1) a poorly representative and poorly siliceous group ($Si < 1$) corresponding to a Fe like-gel effectively observed, 2) a well representative group with $1,5 < Si \leq 2$ corresponding to probable 1:1 structures and 3) a group with $Si > 2$ corresponding to 2:1 or 1:1/2:1 mixtures of phases. Such groupings were also valid when considering total iron as Fe^{3+}.

The 1:1 phases ($1 < Si < 2$)

Octahedral cations numbers (OCN) in the 1:1 phases group were obtained from structural formulae, including Al^{VI}, Fe^{2+}, Mg and Ti contents measured or calculated. Figure 9 represented the variations of the divalent cations ratio in octahedra (Fe^{2+} + Mg/OCN) as a function of the total octahedral cations. Such a diagram clearly shows that the composition of the 7-Å phases was regularly varying from a dioctahedral end-member containing almost 20% of (Fe + Mg) in octahedral layer to a quasi trioctahedral end-member with almost 100% [FE+Mg] in octahedra. The dioctahedral end-member corresponded to very near kaolinite like-phases in which 20% (Fe + Mg) substituted equivalent Al content (Ti was a minor element) and this was until now unknown in natural Fe-Kaolinites.

Generally, no more than 3% Fe_2O_3 was previously found by different methods to accomodate within the octahedral sheet of kaolinites (Petit and Decarreau 1990). The continuity and regularity of plotted values in Figure 9 suggested also that all the different 7-Å phases structurally detected with HRTEM were developed from a same crystallochemical process evolving from an original (Fe-kaolinite) dioctahedral end-member to a pure (Fe + Mg) trioctahedral one. This demonstrated also that many 7-Å crystallites had an intermediate di-trioctahedral composition. To test the possible relationship between the Fe-kaolinite like phase and the 7-Å Fe phase, Fe^{2+} values from the 1:1 Fe phases were first plotted as a function of total Al and a corresponding regression line was then obtained (Figure 10) showing a good negative correlation. Then the Fe and Al values, corresponding to the Fe-kaolinite identified with HRTEM, were plotted on such a diagram only after it was drawn. It is interesting to note

https://doi.org/10.1346/CCMN.1995.0430408 Published online by Cambridge University Press

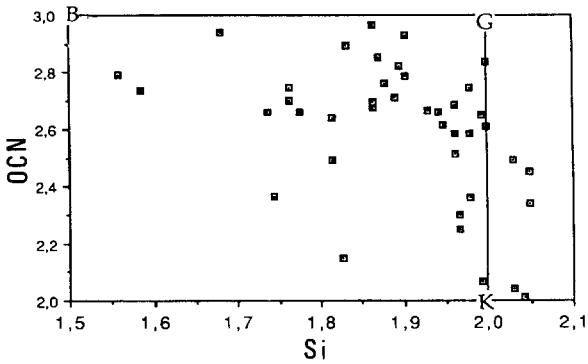

Figure 11. Variations of the octahedral cations number (OCN) as a function of Si content in the 1:1 phases group. The Kaolinite $[Si_2Al_2O_5(OH)_4]$ = K; Greenalite $[Si_2(Fe^{2+}, Mg)_3O_5(OH)_4]$ = G; and Berthierine $[(Si_{1,5}Al_{0,5})(Fe^{2+}, Mg)_{2,5}(Al,Fe^{3+})_{0,5}O_5(OH)_4]$ = B poles are visualized.

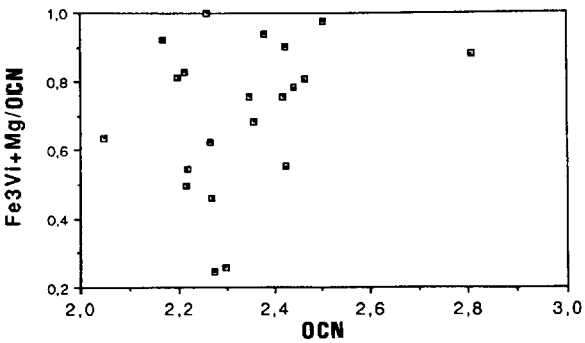

Figure 12. Variations of the $(Fe^{3+}_{VI} + Mg)$ ratio in octahedra as a function of the octahedral cations number (OCN) in the 2:1 and 1:1/2:1 phases.

that such plots were well aligned with the others. Figure 10 revealed a chemical gap between the field of kaolinites and the one of 7-Å Fe phases. It confirmed also that all the 7-Å phases followed the same evolution trend. Concerning the chemical gap, it might be suggestive of a transformation process implying the dissolution of the Fe-kaolinite like phase and the recrystallization of a Fe-rich 7-Å phyllosilicate with a variable composition. This composition was then regularly tending towards an iron richer and richer and Al poorer end-member. Lastly, variability of the Si content was found accompanying the 7-Å kaolinite (dioctahedral) like phase evolution towards the 7-Å Fe rich (trioctahedral) phase.

From Figure 11, it was evident that octahedral and tetrahedral changes occurred during such a transformation, with decreasing Si as OCN increased. These results confirmed that a dissolution-recrystallization process certainly took place inside the evolving 7-Å phases group. This conflicts with the solid state process proposed by Giresse *et al* (1988). Indeed, for these authors, the transformation product of original kaolinite tends towards a greenalite composition $[(Si_2)(Fe^{2+},Mg)_3O_5(OH)_4]$ which needed only octahedral substitution of (Fe + Mg) for Al and preservation of the tetrahedral layer.

The 2:1 and 2:1/1:1 phases (Si > 2)

Concerning the group of phases with Si > 2, a first chemical test similar to that displayed in Figure 9 gave incoherent results. So corresponding structural formulae were calculated again with total iron considered now as Fe^{3+}. Figure 12 shows the variation of the $[Fe^{3+}$ + MG] content in octahedra as a function of OCN. It appeared that all the analytical plots were located in the 2 < OCN < 2,6 field and mainly that, contrary to the 1:1 phases (Figure 9), these plots have a wide spread. Such results suggest that iron present in these phases is not completely (or not at all) Fe^{2+}. This group is chemically heterogeneous and the composite phases of the group do not follow a unique evolving trend. It is also evident from Figure 13 that the K content increased in the structures as this group evolved towards a more and more dioctahedral pole. Such an increase of K revealed the 7/10Å interstratified structures transformed more and more into 10-Å like mica phases. The direction of the evolutive trend in this group (from a trioctahedral to a dioctahedral end member) is the reverse of the 1:1 phases group. Figure 14 confirmed the global heterogeneity of this group and permitted us to hypothesize it was possibly made of 2 coexisting subgroups of originally distinguishable phases which tended to a crystallochemical homogeneity as K content increased. One (Fe + Mg) rich subgroup was probably inherited from the 7-Å (Fe) phases group before it transformed into mica like structures. A second subgroup was originally Al-rich, without any relation with the 7-Å Fe phases, before it experienced the same transformation. As seen also in Figure 14, the Al content increased in the first subgroup and stayed constant in the second during the mica-like transformation process. In both cases, probably, Al released by kaolinite during its transformation into 7-Å Fe phases was used.

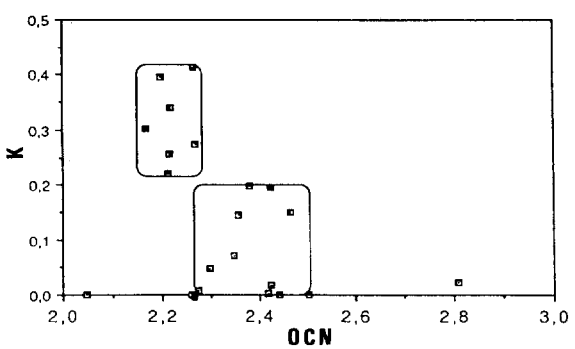

Figure 13. Variations of the K content as a function of octahedral cations number in the 2:1 and 1:1/2:1 phases.

https://doi.org/10.1346/CCMN.1995.0430408 Published online by Cambridge University Press

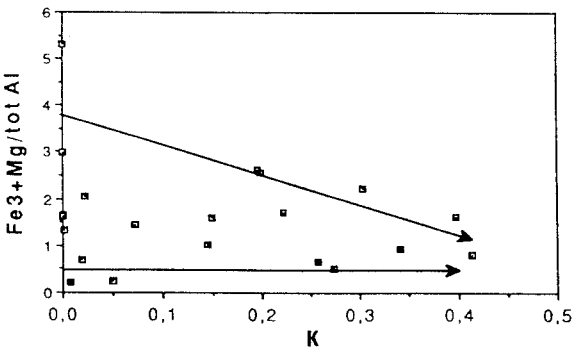

Figure 14. Variations of the (Fe^{3+}_{VI} + Mg/Al_{Tot}) ratio as a function of K content in the 2:1 and 1:1/2:1 phases.

DISCUSSION

Textually, it is interesting to note there are very clear morphological differences between the two 7-Å phases groups observed. Indeed, crystallites illustrated in Figure 5 appeared very thick, generally short, with a regular structure and were very quickly beam-damaged while crystallites illustrated in Figure 3 were thin, flexible, generally elongated and much more beam-resistant. Chemically, the first crystals were identified as kaolinite-like phases and the second as 7-Å Fe phases. This implies that, according to the hypothesis of a kaolinite–7-Å Fe phase transformation with time (Giresse *et al* 1988), such a transformation obligatory took place following a dissolution-crystallization process since there is no one morphological resemblance, no structural inheritance or structural relation between them. This is supported in addition by corresponding chemical results. Indeed a clear and unique evolving trend is evident inside the 1:1 phases group from crystallochemical tests (Figures 9 and 10) and details of Figure 10 which shows the Fe variations of all the 1:1 phases observed as a function of total Al. The data also revealed a chemical gap between the kaolinite-like phases and the 7-Å Fe phases. So it is probable that a chemical discontinuity is accompanying the structural one. It was also evident, from Figure 11, that both octahedral and tetrahedral changes occurred inside the evolving 7-Å phases group which is not easy to realize in the solid-state. It is also interesting that, before the kaolinite-like crystallites experienced a dissolution-recrystallization process, the [Fe + Mg] content was about 20% of the octahedral composition which is original in natural material. (If the primary kaolinites were originally pure or already "iron-rich" is not known from our analyses.)

Concerning the 7-Å Fe–10-Å mica like phases transformation, a solid state mechanism has been clearly evidenced, giving several intermediate interstratified structures and showing lateral transitions in which one 10-Å mica layer replaced one 7-Å Fe layer (Figures 7 and 8). Detailed examination of several images similar to Figure 8 indicated that such transformation may occur mainly via nucleation and growth (insertion) of tetrahedral sheets, at interlayer levels of 7-Å Fe structures, from one or both edges to the core of the crystallites, as already seen in equivalent cases by ourselves (Amouric *et al* 1988, Amouric 1987). (Of course, such a transformation may also start at edge dislocations level which are very numerous in the low-temperature phyllosilicates studies.) Structurally, this mechanism is the reverse of that proposed by Sing and Gilkes (1991) for muscovite to kaolinite weathering (Mode 1). Now to be chemically satisfying, this transformation also needs a simultaneous entrance of K at interlayer levels and partial Al for (Mg + Fe) substitution in octahedra of 7-Å Fe phases. Both these phenomena are presumably possible by ions diffusion from outside, via the growth fronts of the new developing tetrahedral sheets. (Globally, such a reaction is the reverse of that probably implied in the 10-Å (illite) to 7-Å (ferroan lizardite) phase transition observed by Lee and Peacor (1983).) So "the solid-state transformation mechanism" proposed is not strictly a one-as in the great majority of similar cases previously reported in the literature. Rather it is a "solid-state mechanism assisted by diffusion" in transformations in which a great part of the original architecture (structure) is preserved.

If a great part of the 10-Å mica like phase observed was obtained through 7/10Å interstratified sequences, it appeared it was not the only possible mechanism for its genesis. Indeed, some thin and pure 10-Å like mica crystallites, quite different from thicker 7/10Å mixed ones, were also distinguished (Figure 6). We hypothesize such pure 10-Å sequences were directly neoformed, and chemical results support and reinforce this morphological inference. So Figure 12 showing greatly spread out analytical points, revealed that an important chemical heterogeneity globally existed among the group of phases with Si > 2 and Figure 14 also permitted us to propose in fact mica like structures were generated following two different ways: first through 7/10 interstratified sequences (as illustrated in Figures 7 and 8) and the second directly by dissolution of kaolinites and neoformation of K richer and richer mica like-material (as illustrated in Figure 6). In both cases, resulting mica-like structures were also strongly aluminous. Dissolution of primary kaolinites, invoked before, provided such a needed Al.

To obtain coherent (2:1) structural formulae, we were obliged to admit compositional iron existed (partially or globally) as Fe^{3+} in these structures. That means that the (1:1)–(2:1) transitions described before certainly took place in a more oxidizing environment than this needed at the beginning, for the kaolinite–7-Å Fe phase transformation.

Giresse *et al* (1988) have never seen the 10-Å structures we observed and Odin *et al* (1989) have only

reported something rather resembling a "pyrophyllite" obtained by recrystalliztion of 7-Å Fe phases and, this, probably in more ancient and deeper green peloïds that those we have studied here. In our opinion, the 10-Å mica phases we described could be precursors of a glauconization process beginning in recent green peloïds (Parron and Amouric, in preparation).

Lastly this study permitted us to discuss the chemical aspect of the 7-Å Fe phase which, effectively, may occur as a pure and specific mineral. Indeed, it was already clear after Figure 9, that the composition of such a particular phase was varying—in a quasi continuous manner—from a dioctahedral pole (of Fe-kaolinite type) to a trioctahedral one (with almost 100% [Fe + Mg] in octahedra). Figure 15a confirmed the chemical repartition field of the 7-Å Fe phase was very extended, roughly evolving between a (Fe)-kaolinite and a greenalite pole. We did not therefore prefer to give an unsignificant mean structural formula for it. Furthermore it was not possible to determine the oxidation state for Fe with EDX analyses used.

This study has also demonstrated the 191-7G specimen was, in detail, a mixture of several phases (mainly 7-Å Fe phase, + ferriferous gel, + kaolinite, + 10-Å phase, + quartz, + anatase). So the structural formula proposed for the 7-Å Fe phase by Giresse et al. (1988) and obtained with global methods on the same specimen, probably corresponded to a mean analyse of such a mixture! The same holds for Odin *et al* (1988, 1989) which proposed a different formula from similar specimens, also obtained with similar analytical methods. For comparison purposes, we have then calculated a mean structural formula after adding all the analytical results of all the phases detected here and reported it with the mean values given by Giresse *et al* and Odin *et al* for the 7-Å Fe phase on the same diagram (Figure 15b). Calculated on the same basis (total iron = Fe^{2+}, 1:1 structure considered only), these three values appeared very near one another. This definitively demonstrates that the above mentioned studies had, in fact, reported mean values of all the phases effectively intimately mixed, even when the 7-Å Fe mineral was sufficiently dominant in the specimen. This also greatly emphasizes the necessity to use fine-scale analytical methods, which are more precise.

The "young 7-Å phase" seems to be a metastable one. In the 191-7G specimen, it obviously undergoes well documented transformations towards 2:1 structures with changing sedimentation conditions, for example. However we have also observed a quite similar phase in old marine green grains belonging to Paleocene formations (Parron 1989, Amouric and Parron 1992) which we shall compare elsewhere.

CONCLUSIONS

Thanks to HRTEM observations coupled with microanalyses, several major and novel conclusions may be derived from this investigation. A fine mixture of phases (with several species previously unrevealed) was evidenced. Interesting details of intimate structures as precise chemical composition of each main phase were obtained and different transformation mechanisms between phases were proposed. In summary, in the same young green grains observed, original (Fe)-kaolinites with 20% octahedral [Fe + Mg] and di-tri to trioctahedral [Fe + Mg] rich TO phases were structurally and chemically very characterized. Interlayered 1:1/2:1 structures and pure dioctahedral 2:1 (Al, K) rich phases were also detected and studied in detail. Genetically, all these phases are related in the same evolutionary process. Starting from (Fe)-kaolinite, the first stage comprises the dissolution of this specie and the recrystallization of a richer and richer (Fe + Mg) and poorer and poorer Al 7-Å phase which tends toward a trioctahedral pole. An evident structural and, possibly, chemical gap accompanies this stage. If the starting kaolinite involved is a primary pure one or whether it is originally (Fe)-rich is presently unknown. Crystallization of a 10-Å, (Al +K) rich, more and more dioctahedral mica-phase then occurs at the expense of the 7-Å Fe phase, through 1:1 / 2:1 interstratified sequences. Such an evolution takes place through a solid state mechanism in which a 2:1 10-Å layer clearly replaces a 1:1 7-Å layer. Some (2:1) like mica structures may also directly occur by neoformation, after dissolution of kaolinites. During this second stage of transformation, a probable change of the Fe oxidation state (from Fe^{2+} to Fe^{3+}) is needed which indicates a more oxidizing environment exists. The transformation mechanism we deduced from HRTEM and AEM analyses leading to the particular 7-Å Fe phase formation is different from those previously proposed (see Giresse

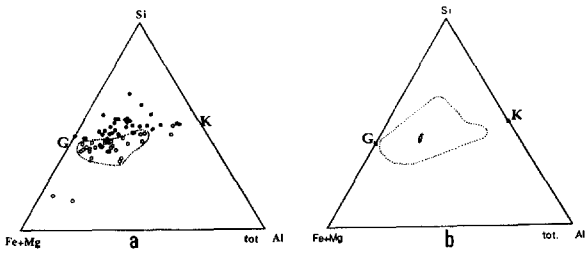

Figure 15. a) Distribution field of all the microchemical analyses concerning the 1:1 and (2:1 + 1:1/2:1) phases in a (Si, Fe^2 + Mg, Al_{Tot}) diagram. K = Kaolinite; G = Greenalite. (O) phases with Si ≤ 2 atoms, (●) phases with Si > 2 atoms. b) Comparison of the mean structural formulae in a (Si, Fe^{2+} + Mg, Al_{Tot}) diagram, concerning respectively: (+) all the analytical points of this study; (O) mean structural formula of the 7-Å Fe phase by Giresse *et al.* (1988) and (●) the mean structural formula for the same phase by Odin *et al.* (1988). All these calculations were done on the same basis (Fe_{Tot} = Fe^{2+}; basal structure = 1:1). K = kaolinite; G = greenalite. □ distribution field concerning the phyllosilicates analyses in this study.

https://doi.org/10.1346/CCMN.1995.0430408 Published online by Cambridge University Press

et al 1988 and Odin *et al* 1988). The frequently observed 7/10Å (K)-rich phases transformation suggests that the glauconitization process is, in fact, beginning in the young green grains studied.

REFERENCES

Amouric, M. 1987. Growth and deformation defects in phyllosilicates as seen by HRTEM. *Acta. Crystallog.* B **43**: 57–63.

Amouric, M., I. Gianetto, and D. Proust. 1988. 7, 10 and 14Å mixed layer phyllosilicates studied structurally by TEM in pelitic rocks of the Piemontese zone (Venezuela). *Bull. Miner.* **111**: 29–37.

Amouric, M., G. Mercuriot, and A. Baronnet. 1981. On computed and observed HRTEM images of perfect mica polytypes. *Bull. Miner.* **104**: 298–313.

Amouric, M., and J. Olives. 1991. Illitization of smectite as seen by HRTEM. *Eur. J. Miner.* **3**: 831–835.

Amouric, M., and C. Parron. 1992. About the glauconitization process. An HRTEM and microchemical study. *Proc. Mediter. Clay Meet.* Lipari 11–12.

Banfield, J. F., and R. A. Eggleton. 1988. Transmission electron microscope study of biotite weathering. *Clays & Clay Miner.* **36**: 47–60.

Casalini, L., M. Amouric, and C. Parron. 1993. Origine et nature d'une phase à 7Å (T.O.) ferrifère: Étude METHR et EDX. Bull. SFMC, vol. 5 n° 3, 58–59.

Cliff, G., and G. W. Lorimer. 1975. The quantitative analysis of thin specimens. *J. Microscopy* **103**: 203–207.

Giresse, P. 1985. Le fer et les glauconies au large du fleuve Congo. *Sci. Geol. Strasbourg* **38**: 293–322.

Giresse, P., A. Wiewiora, and B. Lacka. 1988. Mineral phases and processes within green peloïds from two recent deposits near the Congo river mouth. *Clay Miner.* **23**: 447–458.

Lee, J. H., and D. R. Peacor. 1983. Interlayer transitions in phyllosilicates of Martinsburg shale. *Nature* **303**: 608–609.

Odin, G. S., M. Amouric, S. W. Bailey, and I. D. R. Mackinnon. 1989. Mineralogie du facies verdine. *C.R. Acad. Sci. Paris* **308**: 395–400.

Odin, G. S., S. W. Bailey, M. Amouric, F. Fröhlich, and G. A. Waychunas. 1988. Mineralogy of the facies verdine. In *Green Marine Clays.* G. S. Odin, ed. Amsterdam: Elsevier, 159–206.

Odin, G. S., and P. Giresse. 1972. Formation des Minéraux phylliteux (berthierine, smectites ferrifères, glauconites ouvertes) dans les sédiments du Golfe de Guinée. *C. R. Acad. Sci. Paris* **275**: 177–189.

Odin, G. S., and A. Matter. 1981. De glauconiarum origine. *Sedimentology* **28**: 611–641.

Olives, J., and M. Amouric. 1984. Biotite chloritization by interlayer brucitization as seen by HRTEM. *Am. Miner.* **69**: 869–871.

Parron, C. 1989. Voies et mécanismes de cristallogénèse des minéraux argileux ferrifères en milieu marin: Ph.D. thesis. Marseille, 189 pp.

Petit, S., and A. Decarreau. 1990. Hydrothermal (200°C) synthesis and crystal chemistry of iron-rich kaolinites. *Clay Miner.* **25**: 181–196.

Porrenga, D. H. 1967. Clay mineralogy and geochemistry of recent marine sediments in tropical areas. Publ. Fysich-Geographishes Lab. Univ., Dort-Stolk, Amsterdam, 155 pp.

Sing, B., and R. J. Gilkes. 1991. Weathering of a chromian muscovite to kaolinite. *Clays & Clay Miner.* **39**: 571–579.

Von Gaertner, H. R., and W. Schellman. 1965. Rezente sediments in Küstenbereich der Halbinsel Kaloun, Guinea. *Tscher. Miner. Pet. Mitt.* **10**: 349–367.

(*Received 13 April 1994; accepted 8 August 1994; Ms. 2493*)